Journal of Hazardous Materials 161 (2009) 1255–1264

Contents lists available at ScienceDirect

Journal of Hazardous Materials

journal homepage: www.elsevier.com/locate/jhazmat

A comparative study of natural, formaldehyde-treated and copolymer-grafted orange peel for Pb(II) adsorption under batch and continuous mode

Violeta Lugo-Lugo [a], Susana Hernández-López [a], Carlos Barrera-Díaz [a,*], Fernando Ureña-Núñez [b], Bryan Bilyeu [c]

[a] Universidad Autónoma del Estado de México, Facultad de Química, Paseo Colón intersección Paseo Tollocan S/N, C.P. 50120, Toluca, Estado de México, Mexico
[b] Instituto Nacional de Investigaciones Nucleares, A.P.18-1027, Col. Escandón, Delegación Miguel Hidalgo, C.P. 11801, México, D.F., Mexico
[c] Xavier University of Louisiana, Department of Chemistry, 1 Drexel Drive, New Orleans, LA 70125, United States

ARTICLE INFO

Article history:
Received 26 May 2007
Received in revised form 5 April 2008
Accepted 22 April 2008
Available online 3 May 2008

Keywords:
Biosorption
Orange peel
Lead
Remediation
Water

ABSTRACT

Natural, formaldehyde-treated and copolymer-grafted orange peels were evaluated as adsorbents to remove lead ions from aqueous solutions. The optimum pH for lead adsorption was found to be pH 5. The adsorption process was fast, reaching 99% of sorbent capacity in 10 min for the natural and treated biomasses and 20 min for the grafted material. The treated biomass showed the highest sorption rate and capacity in the batch experiments, with the results fitting well to a pseudo-first order rate equation. In the continuous test with the treated biomass, the capacity at complete exhaustion was 46.61 mg g^{-1} for an initial concentration of 150 mg L^{-1}. Scanning electronic microscopy and energy dispersive X-ray spectroscopy indicated that the materials had a rough surface, and that the adsorption of the metal took place on the surface. Fourier transform infrared spectroscopy revealed that the functional groups responsible for metallic biosorption were the –OH, –COOH and $–NH_2$ groups on the surface. Finally, the thermogravimetric analysis indicates that a mass reduction of 80% can be achieved at 600 °C.

1. Introduction

Heavy metal contamination of water is a serious threat to the globe ecosystem. Strict environmental protection legislation and public environmental concerns drive the search for novel techniques to remove heavy metals from industrial wastewater [1]. Although many techniques have been developed, most are expensive or difficult to implement. However, the use of agriculture waste for biosorption shows great promise. Preliminary economic feasibility studies indicate these natural adsorbents have several advantages over existing technologies, like ion exchange. Biosorbents are inexpensive, easy to chemically modify for increased efficiency, suffer fewer environmental interferences, can be used to recover valuable metals, and can easily be adapted to existing filtration systems [2].

Agriculture is one of the richest sources for low-cost adsorbents. Processing wastes like orange peels posses little economic value and create serious disposal problems [3,4]. Mexico is the 3rd largest orange producer in the world with an annual production of 15 million tons of oranges [5]. The orange processing industry in Mexico produces 600 thousand tons of orange juice, which increases the disposal problem of the residue.

Powdered *Citrus junos* peels have been found to remove almost all Pb(II) from an aqueous solution in a pH range of 4–5.5 up to a maximum capacity of 529 mg g^{-1} [6]. Common orange peels have been used for Ni(II) sorption at pH 6 with a maximum capacity of 158 mg g^{-1} [7]. However, recent work has included modifications to the citrus biomass. In one study, orange peels were saponified with NaOH, then reacted with citric acid, which gave a Pb(II) sorption capacity of 253 mg g^{-1} at pH 4.5–6.0 [8]. In another study, the substitution of phosphate groups onto orange processing residue with Fe(III) produced an effective arsenic sorbent – 70 mg As(V) g^{-1} at pH 3 and 68 mg As(III) g^{-1} at pH 10 [9].

One problem associated with biosorbents is leaching of organic components. Of the methods to increase effectiveness and prevent organic leaching, two seem effective. In one study, pretreating *Sargassum* biosorbent with a 0.2% (v/v) formaldehyde solution increased the metal capacity to 302.5 mg Pb(II) g^{-1}, 87.06 mg Cu(II) g^{-1} and 71.6 mg Ni(II) g^{-1}, at pH 5 [10]. In another study, polyacrylamide was grafted onto coconut coir pith for Cr(VI) sorption with a capacity of 127 mg g^{-1} at pH 3 [11]. Polyacrylamide has been grafted onto other biosorbents, like cotton [12], banana stalks [13], fungal biomass [14], and cellulose [15] with similar success. This grafting method improves the adsorption capacity and also pre-

* Corresponding author. Tel.: +52 722 2173890; fax: +52 722 2175109.
E-mail address: cbarrera@uaemex.mx (C. Barrera-Díaz).

0304-3894/$ – see front matter © 2008 Elsevier B.V. All rights reserved.
doi:10.1016/j.jhazmat.2008.04.087

vents the organic leaching, but also increases the stability of the adsorbent material, which is an important aspect of commercial development of the biosorbent.

Since the effect of formaldehyde pretreatment and graft copolymerization on Pb(II) adsorption by orange peels has not been investigated, these treatments were evaluated in this work using batch and continuous processes.

2. Materials and methods

2.1. Biosorbent preparation (NB)

Orange peels were obtained from a fruit field in the state of Veracruz, México. The peels were rinsed with water, air dried for 5 days, and then crushed and sieved through a 20 mesh screen. The resulting dried biomass was designated as the natural biomass NB.

2.2. Treated biosorbent (TB)

Formaldehyde treatment consisted of mixing 1 g of the NB biomass with 100 mL of a 0.2% (v/v) aqueous formaldehyde solution for 24 h at room temperature. Afterwards, it was filtered and washed with distilled water until no color was detected in the filtrate [10]. The resulting biomass was designated as the treated biomass TB.

2.3. Grafted biosorbent (GB)

The chemical modification of the orange peel consisted of three steps: (a) biomass acidification, (b) copolymer synthesis, and (c) biomass–copolymer grafting.

a. Biomass acidification: The natural biosorbent (NB) was mixed with concentrated acetic acid (98%) in an ultrasonic processor (Ultrasonik^{TM} 28X) at 60 Hz for 30 min. The biomass was separated from the acid solution by decanting and dried in an oven at 60 °C for 24 h.
b. Copolymer synthesis: A copolymer of poly(acrylamide-co-metacrylic acid) in a 0.7:0.3 molar fraction was synthesized by the following process. 0.3 mol methacrylic acid (MAA) and 0.7 mol acrylamide (AA) monomers, were dissolved in acetone and thoroughly mixed at room temperature. Afterwards, 0.05 mL of a 5% solution of benzoyl peroxide in acetone was added as an initiator and the mixture was heated to 70 °C under an N_2 atmosphere for 24 h. The resulting precipitate was washed with acetone, filtered and dried under vacuum for 3 days. The resulting copolymer poly(acrylamide-co-metacrylic acid) was abbreviated as COP.
c. Grafting: For this procedure, 0.5 g COP was dissolved in 25 mL ethanol and 0.5 g of the acidified biomass (step a) was added, along with 0.2 mL of sulfuric acid as a catalyst. The mixture was refluxed for 24 h, and the product was filtered and washed with several portions of warm water to remove the excess copolymer and dried under vacuum. The resulting product was designated as the grafted biomass GM.

2.4. Batch Pb(II) sorption experiments

Adsorption studies were carried out by batch technique to obtain rate and equilibrium data. For these investigations, 0.12 g of adsorbent was added to each of a series of test tubes containing 12 mL of solution with different adsorbate concentrations at pH 5 and agitated intermittently from 0.5 min to 1 h. Equilibrium was achieved quickly in less than 1 h, so shaking for times between 1 and 24 h gave practically the same uptake. Adsorbate initial concentration was 30 mg L^{-1}. This methodology has been previously used [16,17].

At specific times, the test solutions were centrifuged to separate the adsorbent material from the supernate. The solid was dried and characterized using SEM, while the supernate was analyzed for lead concentration using atomic absorption spectroscopy [18]. All experiments were conducted in duplicate.

2.5. Kinetic models and adsorption isotherms

The study of kinetics is an important factor in designing an appropriate adsorption system. The adsorption of heavy metals from the aqueous phase to the solid phase for a batch contact time process, where the rate of sorption of lead onto the surface is proportional to the amount of metal adsorbed, can be well described as a reversible reaction under an equilibrium condition established between two phases. In order to consider the kinetic effects, the Lagergren pseudo-first order equation given by Eq. (1), can be used to determine the rate constant.

$$\frac{dq}{dt} = k_1(q_e - q_t) \quad (1)$$

The values q_e and q_t are the mass of ions adsorbed per gram of sorbent (mg/g) at equilibrium and at time t respectively, k_1 is the rate constant for the pseudo-first order process (min^{-1}), and t is the time (min). In other cases, a pseudo-second order equation may describe the process and it is given by Eq. (2)

$$\frac{dq}{dt} = k_2(q_e - q_t)^2 \quad (2)$$

In this case, k_2 is the rate constant for pseudo-second order sorption (g mg^{-1} min^{-1}) [19].

Furthermore, kinetics effects can be studied using other models, like Eq. (3), the Elovich model [19]. This equation is often valid for systems in which the adsorbing surface is heterogeneous.

$$\frac{dq_t}{dt} = \alpha \exp(-\beta q_t) \quad si \beta >> 1 \quad (3)$$

where α (mg g^{-1} min^{-1}) is the initial adsorption rate and β is related to the extent of surface coverage and the activation energy involved in chemisorption (g mg^{-1}). In this work, pseudo-first, second order kinetics and Elovich model were considered in the study of adsorption process.

The results obtained by the adsorption experiments were analyzed by the models of Langmuir, Freundlich, Sips and Redlich–Peterson. The Langmuir isotherm model assumes uniform energies of adsorption onto the surface with no transmigration of adsorbate in the plane of the surface. The Langmuir isotherm is given by Eq. (4), where q_e is the amount adsorbed (mg g^{-1}), C_e is the equilibrium concentration of the adsorbate (mg L^{-1}), and Q_0 and b are the Langmuir constants related to maximum adsorption capacity and affinity constant, respectively.

$$q_e = \frac{Q_0 b C_e}{1 + bC_e} \quad (4)$$

The adsorption data was also analyzed by the Freundlich model. The Freundlich model is given by Eq. (5), where q_e is the amount adsorbed (mg g^{-1}), C_e is the equilibrium concentration of the adsorbate (mg L^{-1}), and K_F and n are Freundlich constants related to the adsorption capacity and adsorption intensity, respectively [20,21].

$$q_e = K_F C_e^{1/n} \quad (5)$$

The Sips model is a combination of the Langmuir and Freundlich isotherm type models and takes the following form [22]:

$$q = \frac{q_{max} b C_e{}^{1/n}}{1 + b C_e{}^{1/n}} \quad (6)$$

At low sorbate concentrations it effectively reduces to a Freundlich isotherm, while at high sorbate concentrations it predicts a monolayer adsorption capacity characteristic of the Langmuir isotherm. Redlich and Peterson proposed an empirical equation to represent equilibrium data:

$$q_e = \frac{k_R C_e}{1 + a_R C_e^{\beta}} \quad \text{where} \quad \beta \leq 1 \quad (7)$$

where k_R (L g^{-1}), a_R (L mg^{-1}) and β are Redlich–Peterson isotherm constants. This equation reduces to a linear isotherm in the case of low surface coverage and to a Langmuir isotherm when $\beta = 1$ [23].

2.6. Continuous experiments

Fixed bed reactors were used to produce lead sorption breakthrough curves. They consisted of 1 cm diameter glass columns packed with the 0.5 g of TB (selected according to the best results found during the batch experiments). The flow rate was 1 mL min^{-1} at pH 5.0 with initial metal concentrations of 150 and 250 mg L^{-1}. Filtrate samples at specific time intervals were analyzed by atomic absorption spectroscopy to determine the metal concentration [18].

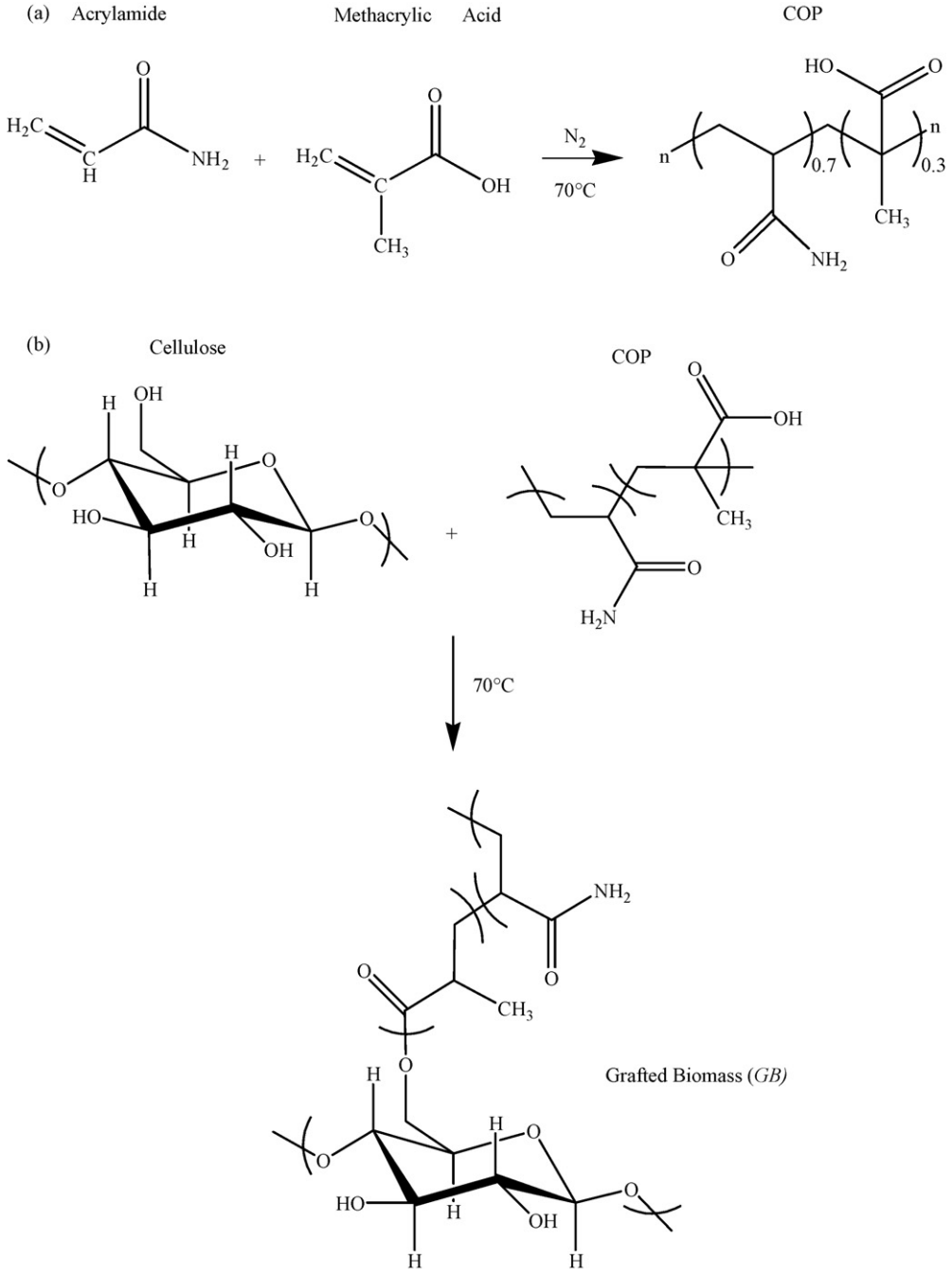

Fig. 1. (a) Copolymerization of acrylamide and methacrylic acid and (b) grafting reaction of COP onto natural biomass NB.

All experiments were conducted in duplicate. The exhausted sorbent was characterized using SEM.

The maximum capacity under continuous flow conditions is described by the Metcalf–Eddy model (Eq. (8)) based on solution concentration and flow [24].

$$q = \frac{(C_0 - (C_e/2))Qt_s}{m} \quad (8)$$

In this equation, q is the sorption capacity (mg g^{-1}), C_0 and C_e are influent and effluent concentration respectively (mg L^{-1}), Q is the volumetric flow (L min^{-1}), t_s is the service time (min), and m is the adsorbent mass (g).

Further, the adsorption isotherms were calculated using 5, 30, 100, 150, 200, 250, 300 and 400 mg L^{-1} concentrations at equilibrium time.

2.7. Characterization

All biosorbents obtained were characterized by the following techniques:

The images of the orange peels before and after adsorption process were captured by scanning electron microscopy (SEM) using a JEOL-5900-LV at 20 keV in *High-vac mode* (with gold sputtering), which included an energy dispersive X-ray probe for semi-quantitative elemental analysis. The UV–vis spectrometry was performed on a PerkinElmer Lambda 25. IR analysis was done on all the biosorbents before and after Pb(II) sorption on a Vertex 70 FTIR spectrometer by ATR. Thermogravimetric analysis was done on a SDT Q600 from TA Instruments in a nitrogen atmosphere at a heating rate of 20 °C min^{-1} from 25 to 600 °C.

3. Results

3.1. Copolymer-grafted biomass

The grafted biosorbent GB was made using a copolymer previously synthesized. This copolymer (COP) was synthesized with thermal induction in order to produced free-radical species that initiates the copolymerization of acrylamide and methacrylic acid through their double bonds (Fig. 1a), with a reaction yield of 99%. It is important to note that one important purpose of the use of these monomers is the incorporation of carboxyl and amide groups onto the cellulose matrix of the orange peel to improve the uptake of Pb(II) and give better stability.

The copolymer was then grafted onto the natural biomass (NB) by an esterification reaction between the hydroxyl groups of the cellulose and the carboxylic acid groups of the copolymer following a condensation mechanism catalyzed by sulfuric acid. The yield of this reaction was 60%. The reaction is shown in Fig. 1b.

3.2. Characterization of biomasses

3.2.1. SEM

The copolymer (COP) obtained in step b (Section 2.3) was a fine white powder with uniform 160 nm diameter spherical particles (Fig. 2a). The SEM micrographs of the biomass before (NB) and after treatment (TB) and after modification (GB) are shown in Fig. 2. In Fig. 2b, the surface of the NB is a continuous cellular arrangement with pores around 20 μm. This orange peel porosity is located in the albedo zone, the white and spongy part of the peel, which consists of enlarged parenchymatous cells with great intercellular spaces, as it shown in micrographs. The orange peel also has a very compact cellular structure, called the flavedo zone containing oil glands and covered with a layer of natural wax. The GB in Fig. 2c has a rougher porous surface morphology which is covered by a layer, indicating the presence of the copolymer on the surface of the biomass. The structure of TB in Fig. 2d is very similar to that of the NB.

This particular cell arrangement of albedo zone allows us to explain the ability of the biosorbents for the impregnation of the pores with external liquid and for remove heavy metals.

3.2.2. FTIR

The adsorption of heavy metals onto any biomass is due to the functional groups on the components [6]. To confirm the

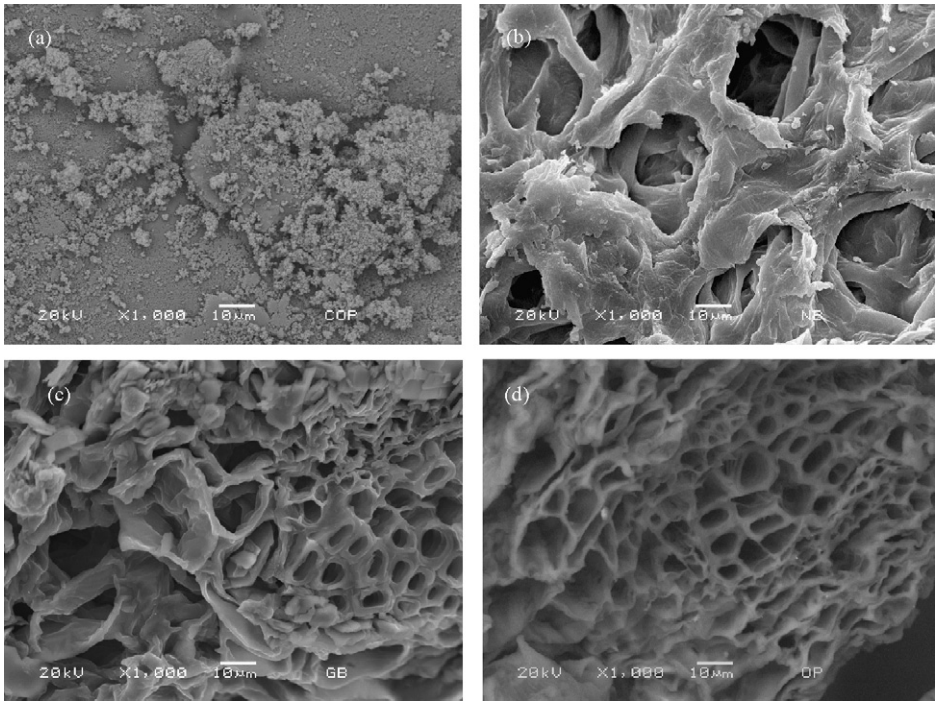

Fig. 2. Scanning electron microphotographs of (a) COP, (b) NB, (c) GB and (d) TB all at 1000×.

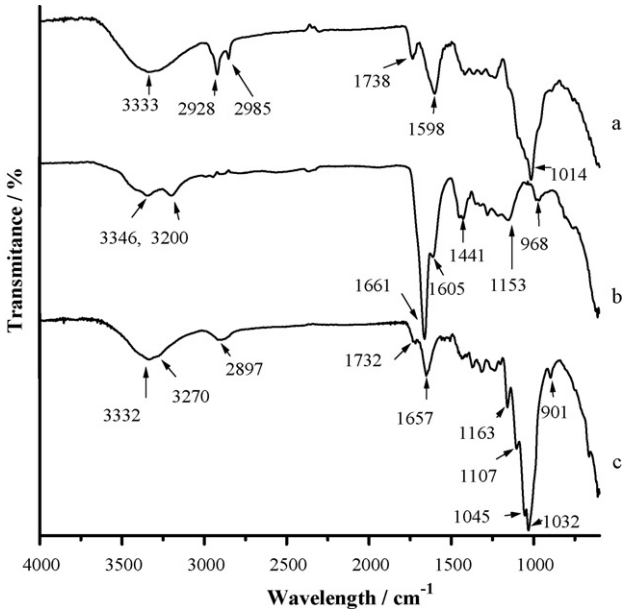

Fig. 3. FTIR spectra of: (a) NB, (b) COP and (c) GB.

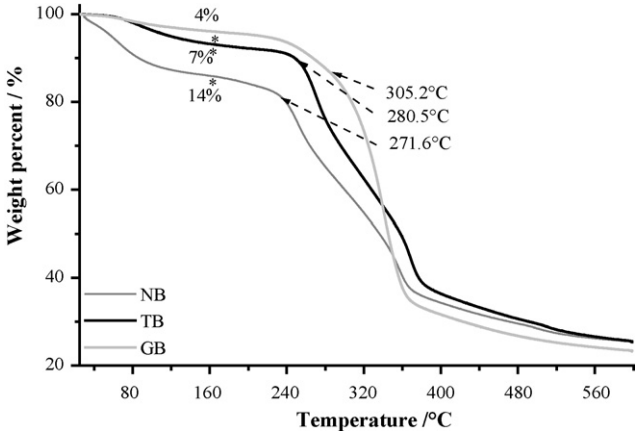

Fig. 4. TGA curves for NB, TB and GB biomass.

modification of the biomass, FTIR spectra were performed on the raw and grafted biomass. Since the NB is mostly composed of cellulose, pectic acid and pectins [7–9] we expect to see the signals due to O–H, C–O, C–H, and C–C bonds in Fig. 3a. The peaks at 3332 are due to –OH vibrations from alcohol and pectic acid components of the biomass. The peaks at 2928, 2985 and 1428 cm^{-1} correspond to the $-CH_2-$ groups in the cellulose; 1738 and 1598 cm^{-1} are assigned to the carbonyl (–C=O) stretching from the carboxylic acid and carboxylate groups, respectively. The broad signal at 1040 cm^{-1} encloses all the vibrations from the C–O bonds in the primary and secondary hydroxyl and the carboxylic acid.

The copolymer (Fig. 3b) is composed of methacrylic acid and acrylamide with the signals corresponding to these groups. The broad doublet from 3550 to 2800 cm^{-1} includes the stretching vibrations of the hydrogen in O–H and N–H groups from carboxylic and primary amide, respectively. The hydrogen-bonded carbonyl from both carboxylic acid and amide appears at 1661 cm^{-1} and the shoulder at 1605 cm^{-1} is the typical N–H stretching from primary amides. Another two important signals are situated at 1441 cm^{-1} (a doublet) and 968 cm^{-1} which correspond to C–H from the methyl and methylene groups and the bending of the OC–OH from the dimer carboxylic acids. After modification of the biomass with the copolymer (Fig. 3c), we can appreciate some important changes that evidence the reaction between carboxylic acid groups from the copolymer and the hydroxyl groups from the biomass. The broad band centered at 3332 cm^{-1} indicates the presence of some hydroxyl unreacted groups and the N–H vibration from the primary amide. The main range in which the most important changes were presented is considered from 1732 to 901 cm^{-1} [11,14,25]. First, signals at 1732 and 901 cm^{-1} show the presence of unreacted carboxylic acids from the copolymer. A new signal appears at 1657 due to the carbonyl stretching from the amide and the hydrogen-bonded new ester group formed during the grafting reaction. Another signal that indicates the presence of the copolymer and the reaction with the biomass, is the split signal centered at 1045 cm^{-1}. This band encloses some bending of C–O, C–O–C and C–N bonds from unreacted hydroxyl (1045 and 1032 cm^{-1}) and carboxylic acid groups, amide (1150 cm^{-1}) and the new ester group (1163 cm^{-1}).

Other work supports these absorption band assignments to functional groups that are expected to be responsible for metallic biosorption, specifically –OH, –COOH and $-NH_2$ groups [26–28].

3.2.3. TGA

A comparison of TGA curves for NB, TB and GB is shown in Fig. 4. The results indicate the best thermal stability is for the grafted copolymer (GB) and TB with respect to NB. For the three samples, the first weight loss measured at 160 °C was: 14% for NB, 7% for TB, and only 4% for GB. This loss is due to the elimination of physically absorbed water and in the case of NB there was an additional loss of some small volatile organic molecules like oils, terpenes, dyes, etc. The second important temperature was the starting decomposition temperature, indicated by rows in Fig. 6. NB has the lower decomposition temperature (271.6 °C) followed by TB (280.5 °C) and GB (305.2 °C). Decomposition temperatures in both of these last samples were improved by 3% (9 °C) and 12% (33.6 °C), respectively from the NB. Those important changes indicate that during chemical treatment there was: (1) a better removal of volatile organic compounds and (2) structural changes due to chemical reactions with formaldehyde and the copolymer giving a better stability. Thus, both TB and GB do not exhibit leaching of organic components like seen in the NB [27].

3.2.4. UV–vis

One parameter that increases the feasibility of industrial use of the biosorbents is the absence of organic leaching from the biosorbent to the aqueous solution which leads to secondary pollution. As we mentioned in Section 1, one method to give biomass stability is the pretreatment of the biomass with formaldehyde. Fig. 5 shows a comparison of UV–vis spectra of the remnant solution from batch sorption. Two absorption bands are prominent, one of them between 300 and 350 nm with a maximum at 319 nm, and another in 250–300 nm with the maximum at 272 nm. They can be attributed to organic compounds, chromophores, and essential oils in the orange peels that absorb in the UV range.

A distinct decrease in absorbance of the remnant solution with modification and pretreatment (50% and 75%, respectively) was observed. These results indicate that during the formaldehyde pretreatment organic compounds are extracted from the biomass surfaces. In orange peels, there are pigments like chlorophyll and carotenes which are soluble in organic solvents. Furthermore, aldehydes like formaldehyde are commonly used for preservation of plant and animal tissues, which gives added stability to the material. As a result, the absorption diminutions of those UV bands

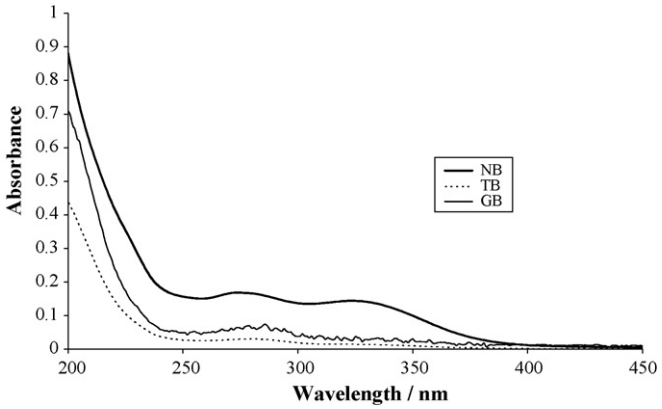

Fig. 5. UV–vis spectra of batch remnant solutions of NB, TB and GB.

observed in the remnant solution after treatment are due to extraction.

Another explanation for the reduction of organic leaching from TB is based on the reaction between the formaldehyde and the hydroxyl groups of the natural biomass forming acetal groups which give structural stability to the biomass [29].

$$2R\text{–}OH + HCHO \rightarrow (R\text{–}O)_2CH_2 + H_2O$$

This effect has been observed in other biomasses and is supported by the TGA curves for NB, TB and GB shown in Fig. 4, since the thermal stability is indicative of the chemical bonding in the material.

3.3. Kinetic studies

The rate of biosorption is a very important factor for design and process optimization in industry. The effect of contact time on the adsorption of lead using NB, TB and GB biosorbents is shown in Fig. 6. It shows that the sorption rate of removal of Pb(II) by all the biosorbents is quite rapid at the beginning of the process and becomes slower as equilibrium is approached. In the case of NB and TB, about 99% of the adsorption capacity for Pb(II) was attained within the first 10 min of contact for a Pb(II) solution of 30 mg L^{-1}. When GB is used, the maximum Pb(II) removal occurs in 20 min. It is observed that in all cases no desorption takes place. Once the equilibrium is reached it remains constant.

The kinetic models of pseudo-first order, pseudo-second order and Elovich model were applied and the calculated kinetic constants, all obtained by a nonlinear regression analysis using the software *Statistica 6.0*, are listed in Table 1. The correlation coefficients obtained for the kinetics models are higher than 0.96 for all biosorbents.

It was found that the pseudo-second order model for NB, TB and GB provides a good description of the experimental data, although the correlations coefficients show that it was not the best fit. The results demonstrate that the amounts of Pb(II) adsorbed at equilibrium were similar for all cases, but highest for TB. Also, the rate constant k_2 for TB (k_2 = 3.02089 g mg^{-1} min^{-1}) was higher than NB and GB (k_2 = 1.8877 g mg^{-1} min^{-1} and k_2 = 0.6681 g mg^{-1} min^{-1} respectively). This can be explained by the existence of functional groups on the surfaces that have been increased as the organics dissolved during the pretreatment.

The pseudo-second order rate expression has been used successfully to describe the adsorption of pollutants from aqueous solutions, and is used to describe chemisorption involving valent forces through the sharing or exchange of electrons between the adsorbent and adsorbate as covalent forces and ion exchange [30].

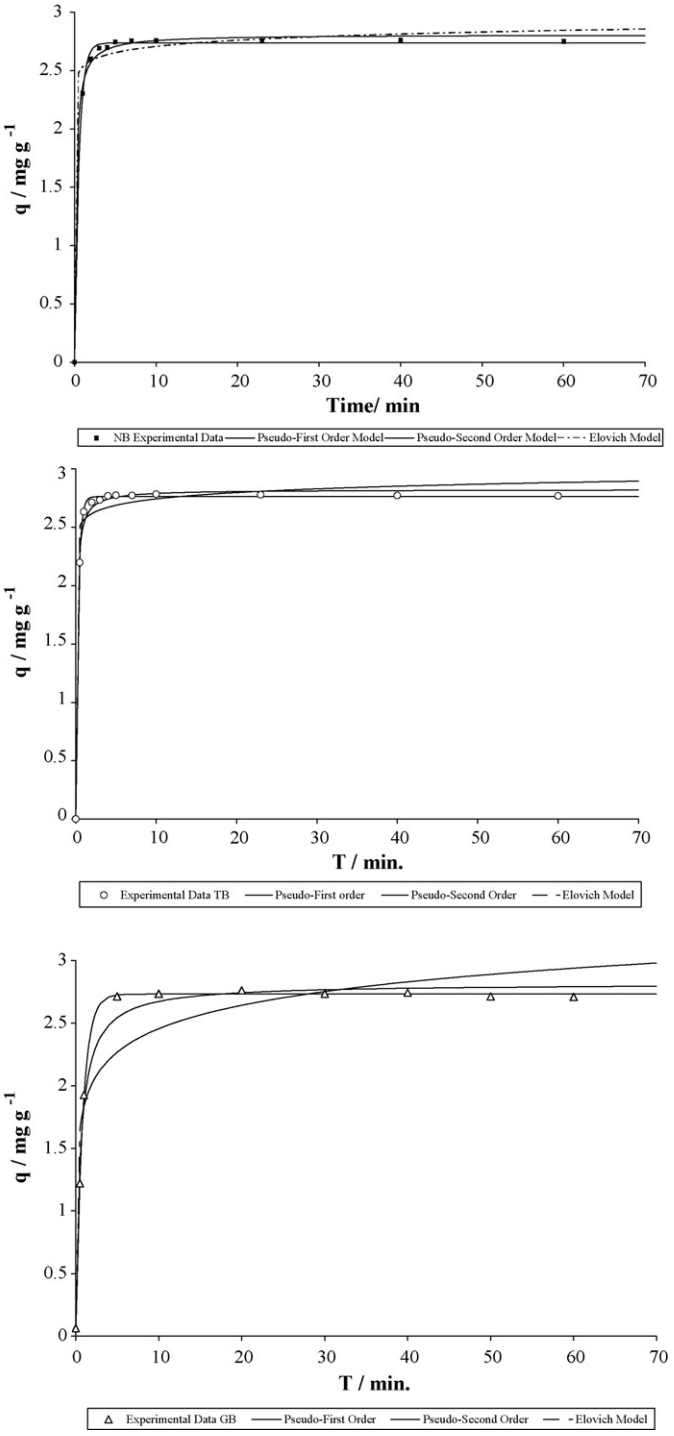

Fig. 6. Lead adsorption by NB, TB and GB as function of time from an initial Pb(II) concentration of 30 mg L^{-1} at room temperature and pH 5.

Although the experimental points could be fitted by the pseudo-second order equation, the best fit was observed with the pseudo-first order model. This model describes reactions at the particle–solution interface, and frequently shows biphasic kinetics with a fast rate at the beginning followed by a slower rate. The experimental data can be described by two first order reactions, behavior interpreted as reactions at two site types: external sites quickly accessible and internal sites which are less accessible [31,32]. The experimental data follow this behavior and Table 1

Table 1
Kinetic constants for the biosorption of Pb(II), pseudo-first, second-order kinetic and Elovich models

	Pseudo-first order			Pseudo-second order				Elovich model		
	k_1 (L min^{-1})	q_e (mg g^{-1})	r^2	k_2 (g mg^{-1} min^{-1})	q_e (mg g^{-1})	h (mg g^{-1} min^{-1})	r^2	α (mg g^{-1} min^{-1})	β (g mg^{-1})	r^2
NB	1.7924	2.7387	0.9994	1.8877	2.8096	14.9011	0.9990	1643×10^{10}	13.0367	0.9933
TB	3.1504	2.7643	0.9997	3.0281	2.8235	24.1400	0.9980	1297×10^{9}	12.7696	0.9884
GB	1.2046	2.7312	0.9996	0.6681	2.8151	5.2941	0.9947	242.7259	3.7084	0.9611

shows that the amount of Pb(II) adsorbed by TB at equilibrium (q_e = 2.7643 mg g^{-1}) is higher than NB and GB (q_e = 2.7387 mg g^{-1} and q_e = 2.7312 mg g^{-1}). Also the Lagergren rate constant k_1 was always highest for TB (k_1 = 3.1504 L min^{-1}). This is indicative of the affinity of the sorbent for the metal being more emphasized for the pretreated biomass.

The correlations obtained for pseudo-first order and pseudo-second order are very close, so it is hard to assume the prevalence of any predominant sorption mechanism. In addition, numerous researches have concluded that the sorption of heavy metals onto biomasses is described by pseudo-second order kinetics.

The Elovich rate equation uses constants for adsorption and desorption to describe the kinetics of chemisorption on highly heterogeneous surfaces. The experimental data in this study do not show as good of a fit as the pseudo-first or pseudo-second order models. However, the results of applying this model to the sorption of Pb(II) on NB, TB and GB show acceptable correlation coefficients with the lowest being r^2 = 0.9611 for GB. This can be explained in function of biomass treatment: NB is more heterogeneous than TB due to the formaldehyde pretreatment and GB is more homogeneous than TB due the grafting of COP onto its surface.As explained in Section 3.2.4, TB biomass does not leach organic compounds during adsorption. Moreover, the number of active binding sites have increased as the organics dissolved. Sample pretreatment can augment adsorption capacity, while avoiding secondary pollution. According to Table 1, the TB biomass has the highest rate kinetic constants. Therefore, the optimum biomass for the continuous process evaluation is TB.

3.4. Biosorption isotherms

3.4.1. pH effect of lead biosorption

The pH of the aqueous solution containing the adsorbate is an important parameter in the heavy metal biosorption processes. Its effect on lead binding was studied by varying the pH of the solution using TB as the biomass. Fig. 7 shows the removal of Pb(II) and the initial and final pH of the aqueous solution. The final pH value was taken from the supernatant solution when the equilibrium time was reached, and the results indicate an increment of the initial aqueous solution pH when the initial pH was 2 or 3, while no changes were observed for pH of 1, 4 and 5.

The increase in the lead binding is likely related to the pH-dependent charges on the surface functional groups like hydroxyl, amide and carboxylic acid. Therefore, the electrostatic attraction plays an important role in metal adsorption onto the orange peels. At pH 2, the positively charged surface of the adsorbent produces an electrostatic repulsion between the surface and the cationic metal. Also, lower adsorption of Pb(II) at strong acidic pH is due to the presence of excess H_3O^+ ions competing with the Pb(II) ions for the adsorption sites.

This is supported by earlier work [8] about the equilibrium, kinetics and isotherm of biosorption of lead ions onto pretreated chemically modified orange peel. As the pH of the system increases, the number of high electronic density sites increases. Electron-rich surface sites on the adsorbent favor the adsorption of metal due to the electrostatic attraction [33].

3.4.2. Initial concentration effect of lead biosorption

The adsorption isotherm studies are of fundamental importance in determining the adsorption capacity of Pb(II) onto the biomass. Four different sorption models are compared for the fitting of experimental data for the lead isotherm of TB at pH 5 and room temperature as shown in Fig. 8.

When the lead concentrations were increased from 5 to 400 mg L^{-1}, the uptake of lead increased too. In order to determine the mechanistic parameters associated with Pb(II) adsorption, the results of the experiments were fit to the Langmuir, Freundlich, Sips and Redlich–Peterson models with the sorption parameters given in Table 2. The fit and all the parameters were also obtained by a nonlinear regression analysis using the software *Statistica 6.0*.

The Langmuir model is probably the most widely applied to sorption isotherms. It considers the sorption energy of each molecule the same, independent of the surface of the material,

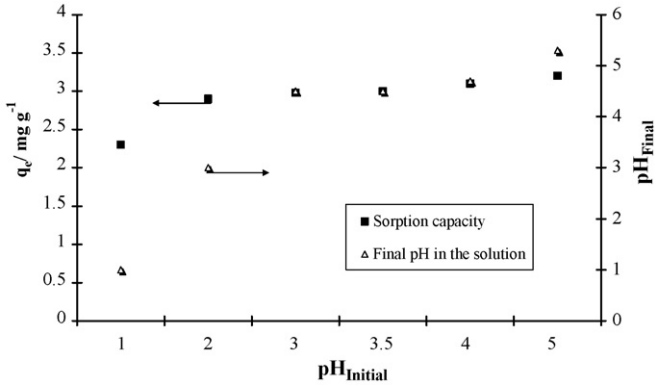

Fig. 7. Lead removal from aqueous solution as function of pH at room temperature for the time to reach equilibrium from an initial concentration of 30 mg L^{-1}.

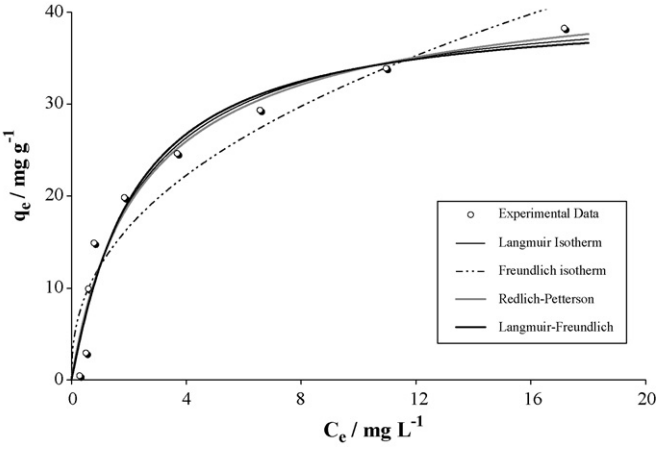

Fig. 8. Adsorption isotherms models for Pb(II) using TB at room temperature and pH 5.0.

Table 2
Isotherm constants for the biosorption of Pb(II) by TB

Q_0 (mg g^{-1})	b (mg L^{-1})		r^2
Langmuir			
41.9981	0.42		0.9768
K_F (mg g^{-1})	n		r^2
Freundlich			
12.4242	2.3813		0.9512
q_{max} (mg g^{-1})	b (mg L^{-1})	n	r^2
Sips			
40.4112	0.443496	0.9345	0.9771
K_R (L g^{-1})	a_R (L mg^{-1})	β	r^2
Redlich–Peterson			
18.9437	0.5121	0.9536	0.9772

with the sorption taking place only on some sites and no interactions between the molecules [34]. This model shows a better fit to the adsorption isotherm data (r^2 = 0.9768) than Freundlich model (r^2 = 0.9512).

The Freundlich model has generally been considered an empirical relationship and has been derived by assuming an exponentially decaying sorption site energy distribution. From Fig. 8 and Table 2, it can be seen that the Freundlich model does not fit the experimental data well. In the low concentration range the calculated Freundlich uptakes are lower whereas in the high concentration range it is higher than the experimental uptake values. Although the Freundlich model has generally been considered an empirical relationship and has been used widely to fit experimental data, it is not the suitable model for describing the lead sorption processes onto TB.

The Sips and Redlich–Peterson models with correlation coefficients of r^2 = 0.9771 and r^2 = 0.9772 respectively, have better fits than the Langmuir and Freundlich models. The overlapped Langmuir, Sips and Redlich–Peterson isotherms are not significantly different, as shown in Fig. 8. In terms of fitting the models to experimental data, it was found that the Sips isotherm model gives a better fit than Langmuir for the lead sorption isotherm of TB. This isotherm model has a simple expression and interpretable parameters in terms of maximum capacity. The materials can be heterogeneous, if the active sites are treated, since the model is based on the heterogeneity of adsorption energy. The parameter n of this model represents the degree of surface heterogeneity – the lower this value, the more heterogeneous the biosorbent sites. The value obtained in this work was 0.9345 [35].

Although the Redlich–Peterson isotherm shows the highest correlations coefficient, the value of β approaches unity (β = 0.9596), indicating that the Redlich–Peterson isotherm tends towards a Langmuir isotherm.

The Langmuir and Sips models are a good fit to describe the lead sorption processes onto TB, because they incorporate an interpretable parameter: Q_0 and q_{max} (41.9981 and 40.4112 mg g^{-1} respectively) which corresponds to the highest possible biosorbents uptake (complete saturation isotherm plateau). Recent papers show the capacity of orange peels for lead and other heavy metals with good fits to a Langmuir isotherm [6–9].

3.4.3. Characterization after biosorption

Once the biosorption was complete, the dried solid was observed using SEM, as shown in Fig. 9. The micrographs show that

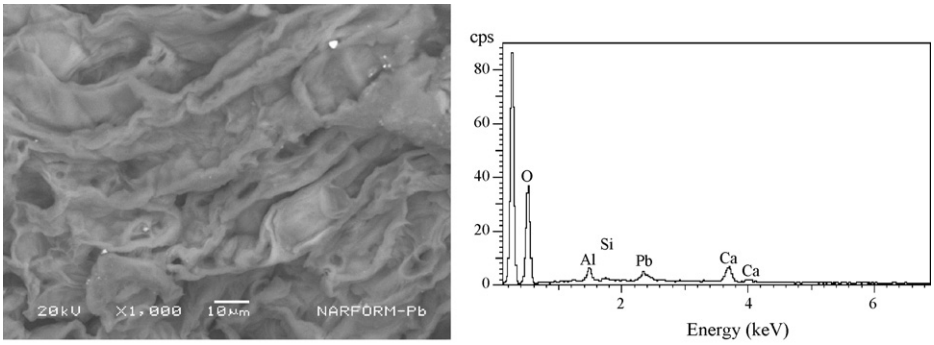

Element	% TB
C	60.0926
O	31.3310
Al	1.5630
Si	3.90x10^{-2}
Ca	3.7466
Pb	3.2278

Fig. 9. SEM micrographs and EDS analysis for Pb(II) using TB.

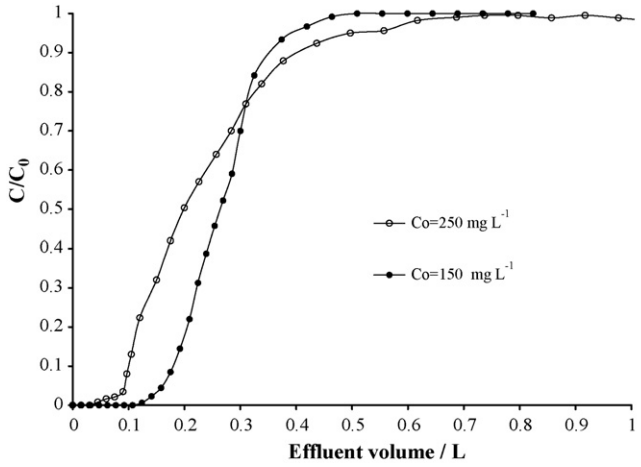

Fig. 10. Breakthrough curves of Pb(II) using TB at room temperature.

Table 3
Service time of the column at different initial aqueous solution concentration

System	Q (mg/g^{-1})	Exhaustion time (min)	Service time (min)
Pb/TB (C_0 = 150 mg L^{-1})	46.61	464	141
Pb/TB (C_0 = 250 mg L^{-1})	22.40	617	60

the TB biomass looks very similar to TB before the sorption process, but with bright edges on the surface, an EDS analysis showed that this corresponds to lead. Moreover particles of calcium and silicon are also evident on the surface.

3.5. Continuous studies

The use of packed bed columns as a reactor for biosorption gives a major advantage because it combines an optimum management of the sorption capacity with very low metal concentration in the effluent. The upper part of the packed biosorbent is saturated at the relatively high incoming concentration of the metal solution so that high uptake values are obtained, whereas the low concentration effluent encounters fresh and powerful sorbent material at the bottom part of the packing. Fig. 10 shows the breakthrough curves of Pb(II) as a function of effluent volume (L). In this work, two initial concentrations were used to evaluate the performance in the continuous system (150 and 250 mg L^{-1}).

Table 3 lists the service time at breakthrough for each concentration. The capacity at complete exhaustion was determined by the Metcalf–Eddy method (where the effluent plot joins the effluent in the breakthrough curve and dividing these values by the weight of adsorbent in the column). The column capacities were found to be greater than their corresponding batch capacities. This effect has been described previously [36].

These are significant results, because column studies have not been done on treated orange peels and are encouraging for applications in industry.

4. Conclusions

There has been an increasing interest in using natural sorbents as well as the pretreatment or chemical surface modification of these sorbents as adsorbents for metal ion removal from aqueous solutions. Surface modification has been a way to enhance the adsorption capacity of many types of sorbents for metal ions. In particular, introducing amino groups on an adsorbent is desirable due to the nitrogen atoms acting as a good chelating agent for the removal of heavy metal ions from aqueous solutions. In this study, natural, formaldehyde-treated, and copolymer-grafted orange peel biosorbents were compared. Using UV–vis spectroscopy, the formaldehyde-treated sorbent showed the least organic leaching into the aqueous solution. In the solution pH values ranging from 2.0 to 6 studied, adsorption amounts for lead ions were greatest at pH 5.0. The Langmuir and Sips adsorption isotherms adequately fit the experimental values. For lead ion removal, the formation of metal complexes with the oxygen atoms in the hydroxyl groups on the surface may play an important role. This pretreated biosorbent has potential applications in water and wastewater treatment for the removal of heavy metal ions since good results were obtained in continuous tests.

Acknowledgements

The authors wish to acknowledge the support given by the Universidad Autónoma del Estado de Mexico, specifically the Facultad de Química (Project UAEM 2425/2007U). Support from CONACYT and supporting research by SNI are greatly appreciated.

References

[1] R. Gong, Y. Ding, H. Liu, Q. Chen, Z. Liu, Lead biosorption and desorption by intact and pretreated *Spirulina maxima* biomass, Chemosphere 58 (2005) 125–130.
[2] B. Volesky, Sorption and Biosorption, BV-Sorbex, Inc., Quebec, Canada, 2003.
[3] G. Selvakumari, M. Murugesan, S. Pattabi, M. Sathishkumar, Treatment of electroplating industry effluent using maize cob carbon, Bull. Environ. Contam. Toxicol. 69 (2002) 195–202.
[4] T.A. Kurniawan, G.Y.S. Chan, W.H. Lo, S. Babel, Comparisons of low-cost adsorbents for treating wastewater laden with heavy metals, Sci. Total Environ. 55 (2005) 402–426.
[5] http://apps.fao.org/faostat. Databases of orange international production and trade (Consulted 01/01/2007).
[6] M. Minamisawa, H. Minamisawa, S. Yoshida, N. Takai, Adsorption behavior of heavy metals on biomaterials, J. Agric. Food Chem. 52 (2000) 5606–5611.
[7] M. Ajmal, R. Rak, R. Ahmad, J. Ajmal, R. Lack, Adsorption studies on citrus reticulata (fruit peel of orange) removal and recovery of Ni(II) from electroplating wastewater, J. Hazard. Mater. 79 (2000) 117–131.
[8] Z. Xuan, Y. Tang, X. Li, Y. Liu, F. Luo, Study on the equilibrium, kinetics and isotherm of biosorption of lead ions onto pretreated chemically modified orange peel, Biochem. Eng. J. 31 (2006) 160–164.
[9] K.-N. Ghimire, K. Inoue, K. Makino, T. Miyajima, Adsorptive removal of arsenic using orange juice residue, Sep. Sci. Technol. 37 (12) (2002) 2785–2799.
[10] J.P. Chen, L. Yang, Chemical modification of *Sargassum* sp. for prevention of organic leaching and enhancement of uptake during metal biosorption, Ind. Eng. Chem. Res. 44 (2005) 9931–9942.
[11] M.R. Unnithan, V.P. Vinod, T.S. Anirudhan, Synthesis, characterization and application as a Chromium(VI) adsorbent of amine-modified polyacrylamide-grafted coconut coir pith, Ind. Eng. Chem. Res. 43 (2004) 2247–2255.
[12] E. Takács, L. Wojnárovits, J. Borsa, J. Papp, P. Hargittai, L. Korecz, Modification of cotton-cellulose by preirradiation grafting, Nucl. Instrum. Methods Phys. Res. B 236 (2005) 259–265.
[13] I.G. Shibi, T.S. Anirudhan, Synthesis, characterization and application as mercury(II) sorbent of banana stalk (*Musa paradisiaca*) polyacrylamide grafted copolymer bearing carboxyl groups, Ind. Eng. Chem. Res. 41 (2002) 5341–5352.
[14] S. Deng, Y.P. Ting, Fungal biomass with grafted poly (acrylic acid) for enhancement of Cu (II) and Cd (II) biosorption, Langmuir 21 (2005) 5940–5948.
[15] N. Bicak, D. Sherrington, B.F. Senkal, Graft-copolymer of acrylamide onto cellulose as mercury selective sorbent, React. Funct. Polym. 41 (1999) 69–76.
[16] V.K. Gupta, M. Gupta, D. Sharma, Process development for the removal of lead and chromium from aqueous solutions using red mud – an aluminum industry waste, Water Res. 35 (2001) 1125–1134.
[17] V.K. Gupta, S. Sharma, Removal of zinc from aqueous solutions using baggase fly ash – a low cost adsorbent, Ind. Eng. Chem. Res. 42 (2003) 6224–6619.
[18] APHA, AWWA, 'Standard Methods for the Examination of Water and Wastewater', 19th ed., American Public Health Association, Washington DC, 1995.
[19] Y.S. Ho, G. McKay, Application of kinetic models to the sorption of copper (II) on to Peat, Adsorpt. Sci. Technol. 20 (2002) 797–815.
[20] V.K. Gupta, Suhas, I. Ali, V.K. Saini, Removal of rhodamine B, Fast Green and methylene blue from wastewater using red mud, and aluminum industry waste, Ind. Eng. Chem. Res. 43 (2004) 1740–1747.

[21] K.P. Singh, D. Mohan, S. Sinha, G.S. Tondon, D. Gosh, Color removal from wastewater using low-cost activated carbon derived from agricultural waste material, Ind. Eng. Chem. Res. 42 (2003) 1965–1976.
[22] R. Sips, On the structure of a catalyst surface, J. Chem. Phys. 16 (5) (1948) 490–495.
[23] O. Redlich, D.L. Peterson, A useful adsorption isotherm, J. Phys. Chem. 63 (1959) 1024–1026.
[24] Metcalf & Eddy, Wastewater Engineering Treatment and Reuse, fourth ed., McGraw-Hill, USA, 2003, pp. 1138–1162.
[25] A. Mishra, A. Yadav, S. Pal, A. Singh, Biodegradable graft copolymers of fenugreek mucilage and polyacrylamide: a renewable reservoir of biomaterials, Carbohydr. Polym. 1 (2006) 58–63.
[26] Y. Sangyun, D. Park, J. Park, B. Volesky, Biosorption of trivalent chromium on the brown seaweed biomass, Environ. Sci. Technol. 35 (2001) 4353–4358.
[27] E. Fourest, B. Volesky, Alginate properties and heavy metal biosorption by marine algae, Biochem. Biotechnol. 67 (1997) 215–226.
[28] A. Selatnia, A. Boukazoula, N. Kechid, M.Z. Bakhti, A. Chergui, Y. Kerchich, Biosorption of lead (II) from aqueous solution by a bacterial dead *Streptomyces rimosus* biomass, Biochem. Eng. J. 19 (2004) 127–135.
[29] J.P. Chen, L. Yang, Study of a heavy metal biosorption onto raw and chemically modified *Sargassum* sp. via spectroscopic and modeling analysis, Langmuir 22 (2006) 8906–8914.
[30] Y.-S. Ho, Review of second order models for adsorption systems, J. Hazard. Mater. B 136 (2006) 681–689.
[31] T. Mathialagan, T. Viraraghavan, Adsorption of cadmium from aqueous solutions by Vermiculite, Sep. Sci. Technol. 38 (2003) 57–76.
[32] D.L. Sparks, Soil Physical Chemistry, second ed., CRC Press, USA, 1999.
[33] M. Arami, N.Y. Limaee, N.M. Mahmoodi, N.S. Tabrizi, Removal of Dyes from colored textile wastewater by orange peel adsorbent: equilibrium and kinetic studies, J. Coll. Inter. Sci. 2 (2005) 371–376.
[34] F. Slejko, Adsorption Technology: A Step by Step Approach to Process Evaluation and Application, Marcel-Decker Inc., USA, 1985.
[35] S.C. Tsai, K.W. Juang, Y.L. Jan, Sorption of cesium on rocks using heterogeneity-based isotherm models, J. Radioanal. Nucl. Chem. 266 (2005) 101–105.
[36] C. Barrera-Díaz, C. Almaraz-Calderón, Ma.T. Olguín-Gutiérrez, M. Romero-Romo, M. Palomar-Pardavé, Cd and Pb(II) separation from aqueous solution using clinoptilolite and *Opuntia* ectodermis, Environ. Technol. 2 (2005) 821–829.